Supplemental Document

Optics Letters

Distinguishing optical and acoustic phonon temperatures of supported 2D materials by nanosecond time-resolved Raman scattering: supplement

MAHYA RAHBAR,[1] IBRAHIM AL KEYYAM,[1] JING LIU,[2] AND XINWEI WANG[1,*]

[1]*Department of Mechanical Engineering, Iowa State University, Ames, Iowa 50011, USA*
[2]*College of New Materials and New Energies, Shenzhen Technology University, Shenzhen, Guangdong 518118, China*
[*]*xwang3@iastate.edu*

Supplement DOI: https://doi.org/10.6084/m9.figshare.26750767

Parent Article DOI: https://doi.org/10.1364/OL.532999

DISTINGUISH OPTICAL AND ACOUSTIC PHONON TEMPERATURES OF SUPPORTED 2D MATERIALS BY NANOSECOND TIME-RESOLVED RAMAN SCATTERING: SUPPLEMENTAL DOCUMENT

MAHYA RAHBAR,[1] IBRAHIM AL KEYYAM,[1] JING LIU, [2,*] XINWEI WANG,[1,*]

[1]*Department of Mechanical Engineering, Iowa State University, Ames, IA 50011, USA*
[2]*College of New Materials and New Energies, Shenzhen Technology University, Shenzhen, Guangdong 518118, P. R. China*
** Corresponding authors: liujing@sztu.edu.cn (J. L.), xwang3@iastate.edu (X. W.)*

1. Physics on distinguishing the OP and AP temperatures of supported nm-thick MoS_2

In Raman-based thermophysical characterization of supported 2D materials, upon photon irradiation, the sample undergoes heating and Raman excitation. If the bandgap of the sample is less than the photon energy, the sample will absorb the laser energy, initiating a cascade of energy transfer among the material's carriers, including hot carriers, OPs, and APs. The process is as follows: initially, electrons within the material absorb the photon energy and are excited from the valence band to the conduction band, leaving holes in the valence band. However, due to the inherent instability of electrons in the conduction band, after a short time (~ns), they recombine with the holes and transfer energy to the OPs through electron-phonon scattering. Subsequently, the energy transfer proceeds from OPs to APs. Given the higher group velocity, heat capacity, and thermal conductivity of APs compared to those of OPs, APs receive nearly all the energy transferred from electrons to OPs. Consequently, they play a dominant role in heat conduction within the sample. This energy-cascading process results in a significant thermal non-equilibrium between OPs and APs [1, 2]. The TMD 2D sample used in this study is MoS_2, characterized by a bandgap of 1.69 eV [3], which is smaller than laser photon energy (2.33 eV). Thus, the energy absorption and cascading mechanism described above apply to our samples.

2. Details on cross-correlation method

The Raman system used in this study consists of a 532 nm CW laser, a Horiba iHR550 imaging spectrometer, and a confocal microscope. Also, a motorized neural density filter wheel (model FW212CNEB) controlled by a LabView program is used to vary the laser power automatically for collecting Raman signals at various P. And the amplitude-modulated CW laser is achieved by modulating the CW laser to a square-wave form using an electro-optic modulator (EOM) (model 350-160, Conoptics) under different frequencies. The $\psi = \Delta\omega/\Delta P = \partial\omega/\partial P$ values are determined using the cross-correlation method [4] rather than the two-step fitting process for establishing the $\omega \sim P$ relationship [5-7]. This global data processing method has significantly improved accuracy and low uncertainty. The cross-correlation equation relating Raman wavenumber with temperature is expressed as

$$G = \sum_{T} \int_{\omega_1}^{\omega_2} I(\omega) \cdot f(\omega)\, d\omega, \tag{S1}$$

where ω_1 and ω_2 define the limits of the range of the Raman peak of interest, $I(\omega)$ is the experimental intensity, and $f(\omega)$ is a Gaussian function given by $f(\omega) = \exp\left[-(\omega - (\omega_0 + \psi P))^2 / C^2\right]$. Here, ω_0 is the Raman peak location at $P = 0$, and C is related to the full width at half maximum. Trial values of ω_0 and ψ, giving the maximum value

of *G*, are taken as the true properties of the Raman spectrum variation versus temperature. More information can be found in our previous work [4].

3. Thickness measurement of MoS_2 samples using atomic force microscopy

In this study, two nm-thick MoS_2 samples are prepared using mechanical exfoliation from bulk material and subsequently transferred onto a Si substrate for the Raman experiments. Details of this mechanical exfoliation process can be found in our previous work [8]. Figure S1 shows atomic force microscopy (AFM) images of the two samples. The experiment is conducted at two distinct locations on sample 1 and one location on sample 2. Analysis of the AFM results reveal a thickness of 25 nm for sample 1 and 10 nm for sample 2.

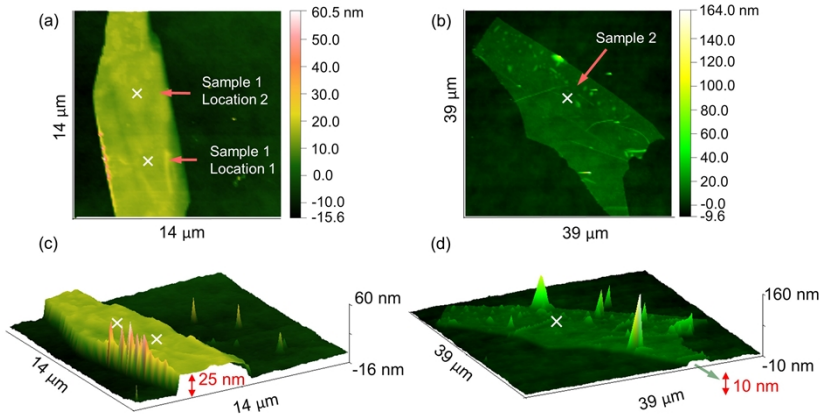

Fig. S1. The AFM images of the two MoS_2 samples studied in this work. Sample 1 with a thickness of 25 nm: (a) top view and (c) side view, and sample 2 with a thickness of 10 nm: (b) top view and (d) side view. The locations where Raman experiment is conducted are shown in the images.

---

4. Applicability of IET model based on objective lens and laser spot size

Figure S2 shows the laser spot size under different objective lenses. As can be seen, as the laser spot size gets smaller, the hot carrier diffusion length (~0.3~0.5 µm) becomes comparable to the length of the laser-heated area. This causes the generated hot electrons to carry heat beyond the laser spot area, where the recombination process transfers energy to optical and acoustic phonons. Moreover, the in-plane heat conduction within the MoS_2 sample becomes more important for smaller laser spot sizes, transporting a considerable amount of absorbed laser energy out of the laser heating area. Consequently, the interfacial energy transfer (IET) model will overestimate interface heat transfer within the laser heating area. However, the 20× objective lens demonstrates a negligible contribution of thermal energy diffusing outside the laser spot area. Further insight into in-plane phonon transport and hot carrier diffusion can be found in the work of Yuan *et al.* [9]. Note that the yellow area represents the sample, and the red area indicates the heat transfer region within the sample and silicon substrate.

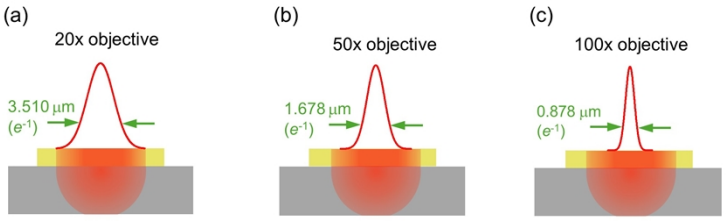

Fig. S2. Laser heating under 20×, 50×, and 100× objective lenses to illustrate the effects of in-plane heat conduction and hot carrier diffusion. The yellow area represents the sample, and the red area indicates the heat transfer region within the sample and silicon substrate. The IET model is applicable only for the 20× objective lens, as the effects of in-plane heat conduction and hot carrier diffusion are negligible in this case.

As discussed in the main paper, for the laser spot size (r_0) measurement, we use the Gaussian beam's radial distribution as $I = I_0 \exp\left(-r^2/r_0^2\right)$, where I is the intensity of the beam at the distance r from the beam center, and I_0 is the maximum intensity of the beam at the center. At the point where the radius equals r_0, the laser intensity is e^{-1} (36.8%) of the maximum value, as shown in Fig. S2. In the past, various methods for defining the laser spot size are found in literatures. Some methods use the distribution of $I = I_0 \exp\left(-2r^2/r_0^2\right)$, and the spot size r_0 corresponding to the location where the intensity drops to e^{-2} (13.5%) of the maximum value [10-12]. Others use the full width half maximum (FWHM) definition, which defines the laser spot size between two points where the intensity is half of its maximum value [13]. And some studies use the same definition as this study [14]. Our definition results in a smaller laser spot size compared to the e^{-2} definition, as shown in Fig. S3. However, all data processing in this paper has been conducted using the same definition, ensuring consistency and not impacting the results. This approach is standard practice within our research group.

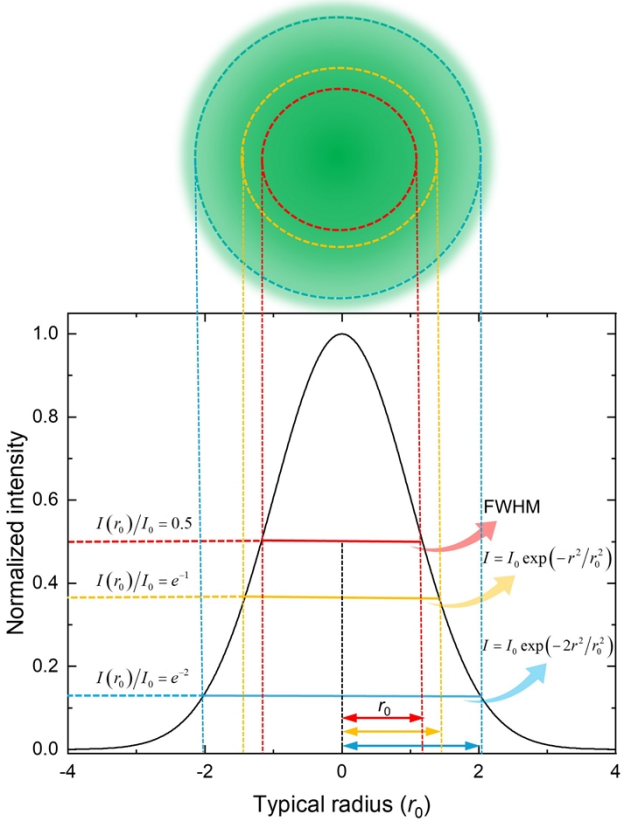

Fig S3. Illustration of different definitions for determining the laser beam radius based on the Gaussian beam intensity profile. I is the intensity of the beam at the distance r from the beam center. I_0 is the maximum intensity of the beam at the center (normalized to 1), and r_0 is the laser spot radius, where the intensity of the beam drops to a certain value.

References

1. N. Hunter, N. Azam, H. Zobeiri et al., Adv. Mater. Interfaces **9**, 2102059 (2022).
2. S. Xu, N. Hunter, H. Zobeiri et al., Mater. Today Phys. **27**, 100816 (2022).
3. K. Kam, and B. Parkinson, J. Phys. Chem. **86**, 463-467 (1982).
4. N. Hunter, M. Rahbar, R. Wang et al., Opt. Lett. **47**, 6357-6360 (2022).
5. H. Zobeiri, N. Hunter, N. Van Velson et al., Nano Energy **89**, 106364 (2021).
6. H. Zobeiri, R. Wang, T. Wang et al., Int. J. Heat Mass Transf. **133**, 1074-1085 (2019).
7. N. Hunter, N. Azam, H. Zobeiri et al., ACS Appl. Mater. Interfaces **12**, 51069-51081 (2020).
8. R. Wang, T. Wang, H. Zobeiri et al., Nanoscale **10**, 23087-23102 (2018).
9. P. Yuan, C. Li, S. Xu et al., Acta Mater. **122**, 152-165 (2017).
10. S. Guenther, M. Koestler, O. Schulz et al., Int. J. Mass spectrom. **294**, 7-15 (2010).
11. T. W. Ng, S. Foo, and H. Tan, Rev. Sci. Instrum. **76** (2005).
12. M. Bonnett Del Alamo, C. Soncco, R. Helaconde et al., AIP Advances **11** (2021).
13. I.-K. Hsu, M. T. Pettes, A. Bushmaker et al., Nano Lett. **9**, 590-594 (2009).
14. W. Cai, A. L. Moore, Y. Zhu et al., Nano Lett. **10**, 1645-1651 (2010).